

# Application of non-destructive optical techniques in the detection of surface and sub-surface defects in sapphire

Ikerionwu A. Akwani\*, Douglas L. Hibbard#, Keith T. Jacoby  
Exotic Electro-Optics (EEO), 36570 Briggs Road, Murrieta, CA

## ABSTRACT

Advancements in optical manufacturing and testing technologies for sapphire material are required to support the increasing use of large aperture sapphire panels as windscreens for various electro-optical system applications. It is well known that the grinding and polishing operations employed to create optical surfaces leads to the introduction of surface stress and sub-surface damage which can affect critical opto-mechanical performance characteristics such as strength and durability. Traditional methods for measuring these defects are destructive and, therefore, unsuitable as in-process, high volume inspection tools. A number of non-destructive optical techniques were investigated at Exotic Electro-Optics under funding by the Office of Naval Research and the Air Force Research Laboratory including Raman spectroscopy, laser polarimetry and the Twyman effect to characterize process-induced defects in sapphire panels. Preliminary experimental results using these techniques have shown that surface stress and sub-surface damage may be non-destructively measured. Raman spectroscopy has shown promise in quantifying surface stress, laser polarimetry is of questionable utility and the Twyman effect may be used qualitatively to monitor relative stress and sub-surface damage. This information will ultimately provide a better understanding of the overall manufacturing process leading to optimized process time and cost.

**Keywords:** sapphire, sub-surface damage, stress, Raman spectroscopy, piezospectroscopic, Twyman, birefringence, polarization

## 1. INTRODUCTION

Optical fabrication processes such as grinding and polishing operations lead to the creation of surface and sub-surface damage. These defects degrade the strength and the performance of functional materials. In order to optimize thermo-mechanical performance, the damaged layer must be identified and minimized or eliminated by subsequent process steps.

Traditional testing methods for measuring surface stress and sub-surface damage include ball indentation testing, cleaving and cross-sectional analysis, and wedge-polish-etch testing, which are all destructive tests.<sup>1, 2, 3</sup> The basic goal of this study was to identify methods capable of quantifying surface stress and sub-surface damage using non-destructive approaches. More specifically, three methods were investigated to determine the most applicable as a large sapphire panel stress and defect mapping tool – Raman / fluorescence spectroscopy, birefringence and the Twyman effect.

To evaluate the application of the non-contact techniques to surface stress characterization, a set of a-plane sapphire panels were characterized by measuring the surface roughness, surface microstructure, stress and defects using Raman spectroscopy, optical polarization, and Twyman effect bowing before and after processing. The sample set was composed of a subset of twelve specimens with ground surfaces and a subset of twelve polished specimens. Each sample was prepared using a different set of processing conditions. The objective in this set of experiments was two-fold: (a) to identify a basic change in signal associated with the grind or polish processing and (b) to quantify the differences between individual specimens and begin to correlate those differences to changes in the processing parameters.

\*iakwani@exotic-eo.com; phone 951-926-7670  
#dhibbard@exotic-eo.com; phone 951-926-7704

Ikerionwu A. Akwani, EEO; Douglas L. Hibbard, EEO; Keith T. Jacoby, EEO; "Application of nondestructive optical techniques in the detection of surface and subsurface defects in sapphire," Window and Dome Technologies and Materials X, Randal W. Tustison, Volume 6545, Page 65450J, 2007 Copyright 2007 Society of Photo-Optical Instrumentation Engineers. One print or electronic copy may be made for personal use only. Systematic reproduction and distribution, duplication of any material in this paper for a fee or commercial purposes, or modification of the content of the paper are prohibited.

<http://dx.doi.org/10.1117/12.720120>

## 2. EXPERIMENT AND RESULTS

### 2.1 Raman / fluorescence spectroscopy

Raman spectroscopy is a well known optical method of characterizing material properties including stress. The technique employs the illumination of a sample with a monochromatic light beam and the subsequent collection and interrogation of the scattered light. The Raman effect involves the shifting of the frequency of scattered light with respect to the excitation frequency. The Raman shift is extremely sensitive to the atomic environment such as the type of atoms and nature of bonding between them. The practical difficulty in using the Raman technique to evaluate stress in a material containing a fluorescing atom is that the intensity of the Raman line is low. A slightly alternative method of measuring stress in sapphire is to exploit the piezospectroscopic effect as applied to the fluorescence from the trace  $\text{Cr}^{3+}$  impurities. Like Raman, the basis of this method is that the characteristic fluorescence lines, commonly known as the R1 and R2 lines, shift under applied stress. The effect of the stress is to distort the lattice environment surrounding the  $\text{Cr}^{3+}$  ions and change the transitional energy between the electronic or vibrational states. This technique has been employed to measure residual stress in sapphire.<sup>4,5</sup>

Specimens were fabricated from commercially obtained a-plane sapphire from Saint-Gobain Crystals. Two sets of sample dimensions were used: 4" x 4" x 0.24" and 9" x 13" x 0.24". The processing and measurements were performed perpendicular to the a-plane surface. Fluorescence measurements were carried out using a LabRam J-Y spectrometer with an 1800 gr/mm grating at room temperature. A HeNe laser excitation source at 632.8 nm wavelength in an optical microprobe was used. Spectra were collected via backscattering geometry ( $180^\circ$ ) at a lateral resolution of 1  $\mu\text{m}$ . 6 mW of incident power was applied to the samples. The low power was necessary to avoid laser heating of the sample since the fluorescence lines are sensitive to temperature. In order to determine the local variation of stress across each sample, three measurements were made on each sample at specified spots before processing and then after processing (both at the same locations). The spectra were band-fitted with two Lorentzian-Gaussian bands to facilitate identification of the exact location of the peak positions contributing to the spectrum, as shown in Figure 1. The lines appearing at  $1368.5\text{ cm}^{-1}$  and  $1398.4\text{ cm}^{-1}$  are the characteristic R1 and R2 lines, respectively.

Figure 1 shows a representative set of spectra illustrating the actual shift of the peaks before and after surface grinding of a sample. The observed frequency shifts attributed to the fabrication process are shown in Figures 2 and 3 for grinding and polishing operations, respectively. The line shift is dependent only on the process-induced stress applied along the crystallographic a-axis and not on previous residual stress. In general, the results show that different processing parameters affect the R-line frequencies. The R-line shifts are analyzed in terms of the difference between the R1 and R2 line shifts, that is, the change in R1-R2 separation as described by He et al. and Sharma et al.<sup>6,7</sup> The resolution of the individual measurements was  $\pm 0.04\text{ cm}^{-1}$ . Comparing that value to the observed peak shifts, it appears that a measurable shift associated with fabrication process induced deformation or stress is observed. Depending on the specific process parameters and the position on the sample where the measurements were made, the shift/stress can either be compressive or tensile. This result is consistent with observations reported by Molis and Clark<sup>8</sup> who measured the complex stresses around indentations in chromium-doped sapphire. It is interesting to note the differences between the grinding and polishing results. Figure 2 shows a predominantly tensile shift which is indicative of localized micro-fracturing. Conversely, Figure 3 shows a combination of tensile and compressive shifts, suggesting plastic deformation and surface micro-cracking. The present results clearly suggest some specific operating parameters that can lead to reduced residual stress levels in sapphire windows.

To further investigate the apparent localized stress variation across a sample, the measurement spots on several specimens were microscopically surveyed. A representative optical photomicrograph of a sample surface is shown in Figure 4. It is clear from the photomicrograph that the surface structure is non-uniform across the sample in agreement with the Raman results.

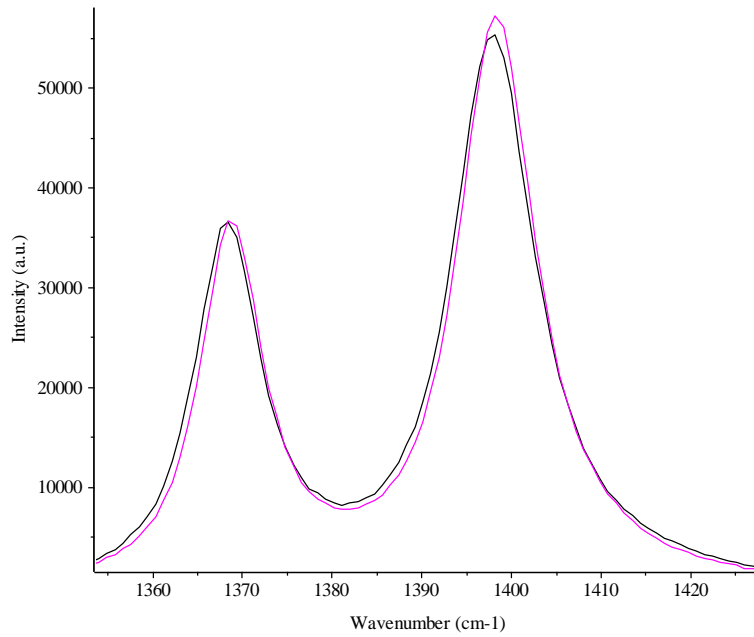


Fig. 1. A representative set of spectra illustrating the actual shift of the peaks before and after surface grinding of a sapphire specimen.

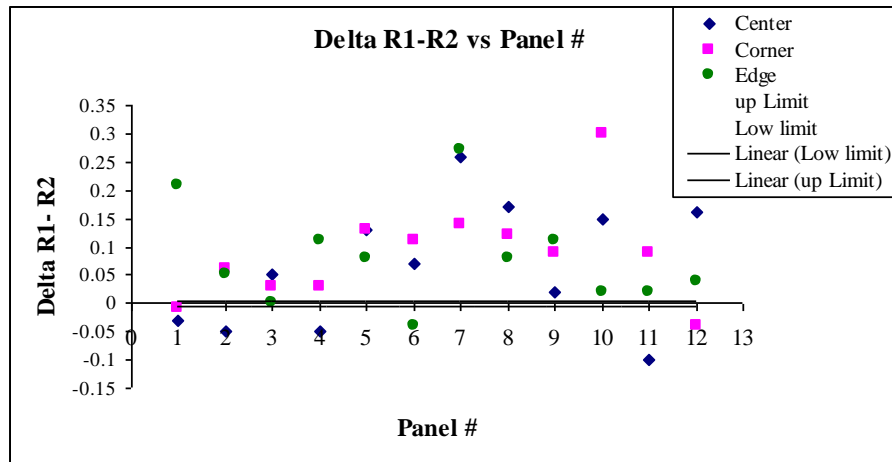


Fig. 2.  $\Delta R1-R2$  line shifts of ground sapphire versus specimen (panel) number.

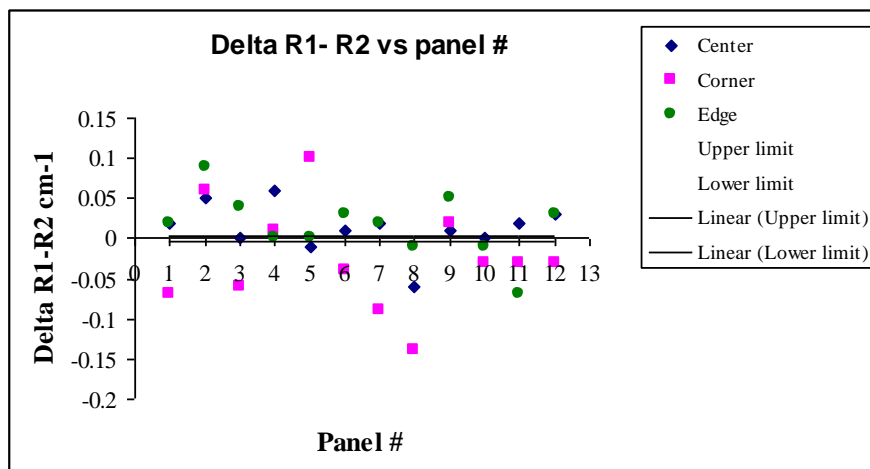


Fig. 3.  $\Delta R1-R2$  lines shifts of polished sapphire versus specimen (panel) number.

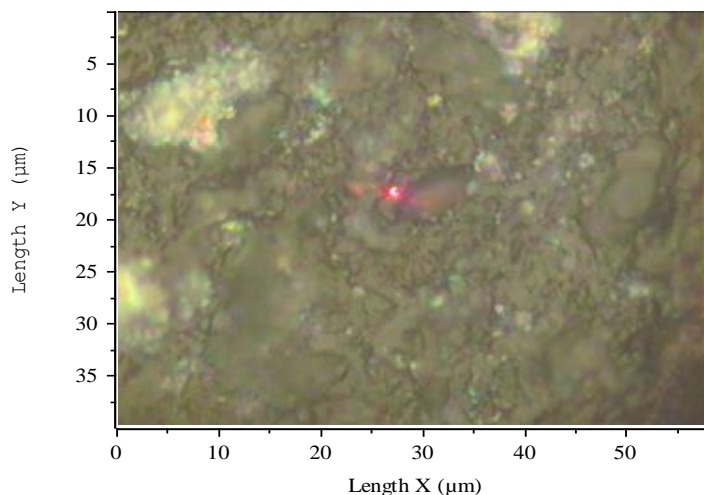


Fig. 4. A representative photomicrograph of a ground sample surface showing localized variation in surface structure.

## 2.2 Optical birefringence (retardation)

Optical polarization based methods are also well established means of characterizing materials. In this case, the technique involved measuring the relative retardance of two orthogonal linearly polarized light rays as they pass through a sapphire panel. The observed birefringence effect is also sensitive to the stress state of the material. As such, the measured level of birefringence could then be used to quantify stress in the panel. The relationship between retardance and birefringence is given by:

$$\text{retardation} = t(n_e - n_o) \quad (1)$$

and the corresponding phase difference is:

$$\Delta\phi = (2\pi/\lambda_0)t(n_e - n_o) \quad (2)$$

where  $t$  is the thickness of the sapphire panel in nm and  $n_e$  and  $n_o$  are the refractive indices of the extraordinary and ordinary rays, respectively, and  $\lambda_0$  is the vacuum wavelength.

Optical retardation measurements of the specimens were performed using a Hinds Instruments Excior system. The results showed large variability in the retardance value. Since the technique measures the integrated retardation effect along a light path passing through the sample, the large variability observed in the retardation values within samples could be due to any one or a combination of the following factors: (a) the total thickness variation; (b) material inhomogeneity; (c) crystal misalignment and (d) perturbation in optical properties due to stress. However, the only factor of interest is the mechanically induced stress due to manufacturing and fabrication processes of the sapphire panels. In this case, by taking a before-fabrication versus after-fabrication snapshot of the birefringence, any lateral inhomogeneities in the material and crystal misalignments should be accounted for. However, the present methodology cannot distinguish individual contributions to overall retardation due to thickness variation and residual stress.

Given this situation, the natural question to ask is how this technique can be used for quantitative stress characterization in sapphire panels. To answer this question, it is important to point out that the retardance is measured in nanometers (nm), implying that a small variation in thickness would significantly affect the retardation values. Figure 5 shows the results of measuring a pre-polished a-plane sapphire specimen. The 3D birefringence results show a very high mean retardation value of 145.934 nm with a standard deviation (STD) of 84.808 nm. If one assumes uniform substrate thickness, the wide range of retardance values from 18.19 to 315.357 represents stress variations within the panel. An examination of the optical photomicrograph (Figure 5-b) of the specimen surface reveals non-uniform scratches which may contribute to the lateral variations in the measured retardance across the sample. This result is consistent with the surface roughness measurements shown in Figure 5-c. These data suggest that the large variability of the retardance observed in this measurement may be principally attributed to thickness variation across the sample.

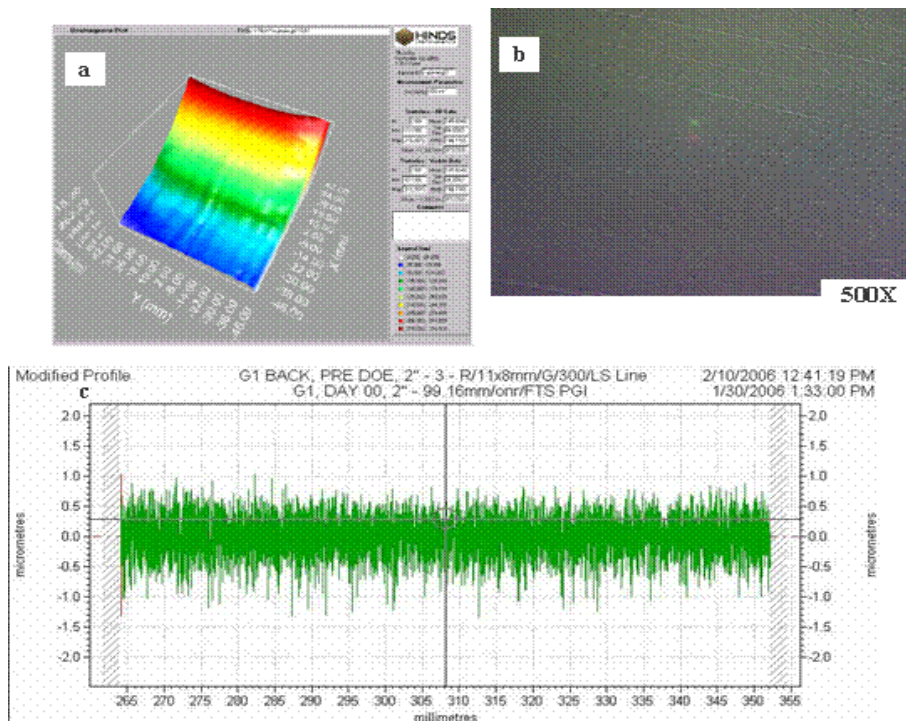


Fig. 5. (a) 3D birefringence: mean value is 145.934 nm, STD is  $\pm 84.808$  nm and range 18.19-315.357 nm; (b) optical photomicrograph showing non-uniform scratches which may lead to corresponding variations in retardance across the sample; (c) variation in surface roughness of pre-polished a-plane sapphire: RMS value is 0.2852  $\mu\text{m}$  and P-V is 2.3701  $\mu\text{m}$ .

To verify this concern, the sample was re-polished for an additional 160 hours and re-characterized. The results are shown in Figure 6. The measured average retardation across the sample was now 33.318 nm with a smaller STD of 11.1234 nm and a narrower range of 0.6564-59.643 nm, as shown in Figure 6-a. Figure 6-b shows an optical photomicrograph of the polished surface with visible pits. This pitting may also contribute to the observed variation in retardance. Figure 6-c shows the surface roughness at different locations on the sample, indicating variations in the sample thickness, which would be expected to manifest itself as variation in the observed retardance. Comparison of the surface roughness measurement as a function of polishing days clearly supports the smoothing of the surface of the sample leading to more uniform thickness (retardance) values (see Figure 6-c).

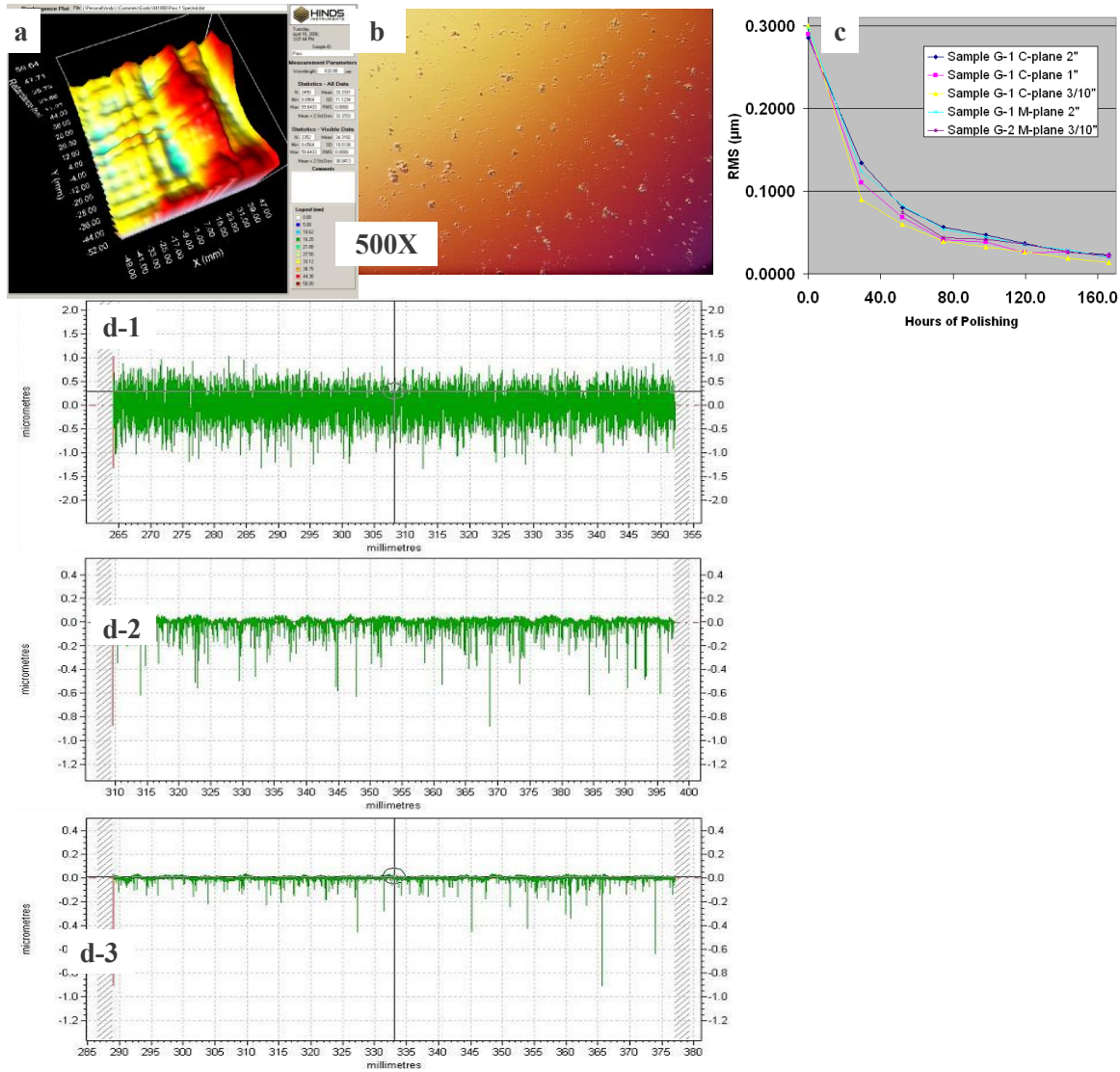


Fig. 6. (a) 3D birefringence result after 160 hours of polishing. The measured average retardation is 33.318 nm, STD is  $\pm 11.1234$  nm, range is 0.6564-59.643 nm; (b) photomicrograph of a polished a-plane sapphire surface; (c) surface roughness as a function of polishing hours (data taken at 3 different locations indicating variations in sample thickness); (d) comparison of surface roughness measurements of a-plane sapphire: (d-1) before polish, (d-2) after 4 days of polish, and (d-3) after 7 days of polish.

It is clear that retardance is determined by local variation in thickness or birefringence or both. In order to confirm the sensitivity of measured retardance to slight thickness variations, the optical retardation results were compared to optical interferometric results. Both techniques are a measure of the optical path length. Figure 7 shows this comparison. From Figure 7, it is evident that the consistency in signal variation across the sample implies that the thickness variation dominates the total birefringence signal with more subtle variation due to stress. More work is needed in this area to allow independent determination of crystal thickness accurately in order to extract the induced birefringence.

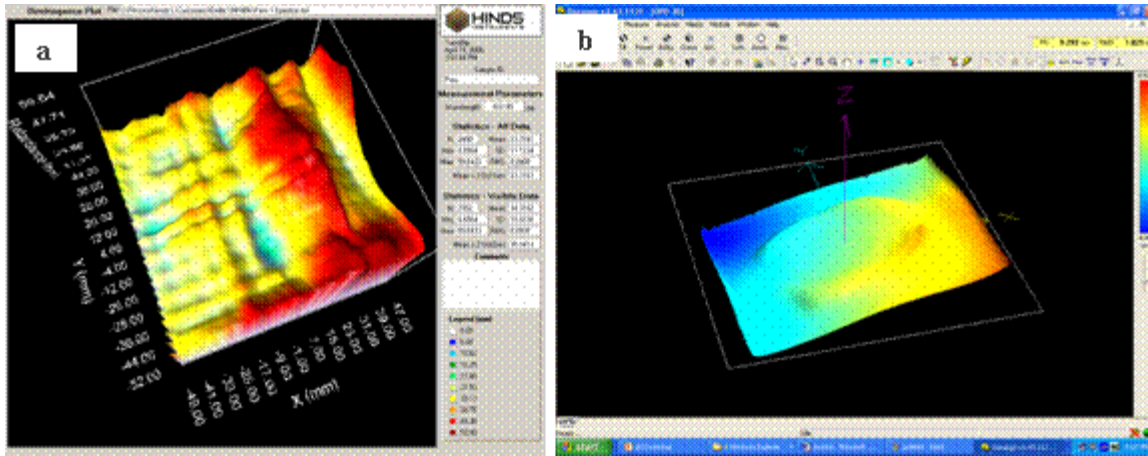


Fig. 7. Comparison of retardation and thickness variation of a-plane sapphire specimen after 160 hours of polishing operation: (a) 3D birefringence result, (b) optical interferometric measurement of thickness variation across sample (optical path length differences). Note the orientations of the two images are the same.

### **2.3 Twyman effect**

The Twyman effect is the bending of a ground/polished plate due to grinding-induced surface stress. The induced stress can be quantified by measuring the curvature of the plate before and after grinding/polishing, typically using an interferometric technique, and relating the curvature to the Twyman constant. Observation of the Twyman effect is usually reserved for thin samples that allow for substantial bowing. Because of the high stiffness of sapphire and the thickness of the panel material, significant stress is required to produce measurable deflection in sapphire panels. However, the data will show that this simple technique is clearly capable of useful qualitative measurement of grinding process-induced stress levels in sapphire panels.

In these experiments, the stress induced during each step of the grinding process was observed when moving from one grinding grit size to the next by measuring the contour of the polished back surface of the sample as the front surface was ground through the sequence of grinding steps. The baseline comparison was done with the back of each sample ground and polished flat per standard EEO processes and as-received from the material vendor on the front surface. The change in surface contour over a 4-inch aperture of the polished back surface was measured as the front surface was ground. The change in contour should be due to the differing stress on the part over the average radial diameter.

Figure 8 shows a series of surface contours illustrating the effect on a representative specimen being ground through a sequence of progressively finer grit sizes. Grit sizes were in the following size progression: A>B>C>D>E. Notice the decrease in the number of fringes as the size of the grit decreases. These results show that sample bow was reduced with the progressive decrease in grit size suggesting that both the total stress and the depth of stress diminished. It is important to note that the measurement includes stress contributions from (a) the grinding operation, (b) blocking during polishing, and (c) holding the part during testing. The change of stress due to holding the part was minimized to less than the resolution of the instrument. Therefore the measured Twyman effect is principally the sum of the stress from blocking and grinding operations.

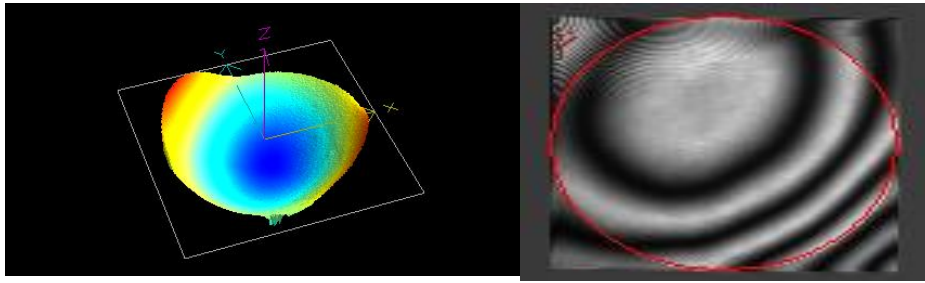


Fig. 8 (a). Surface contour over 4" diameter and interferogram of 4" square surface before grinding: PV 0.9563 wv; RMS 0.2185 wv; Power 0.6852 wv.

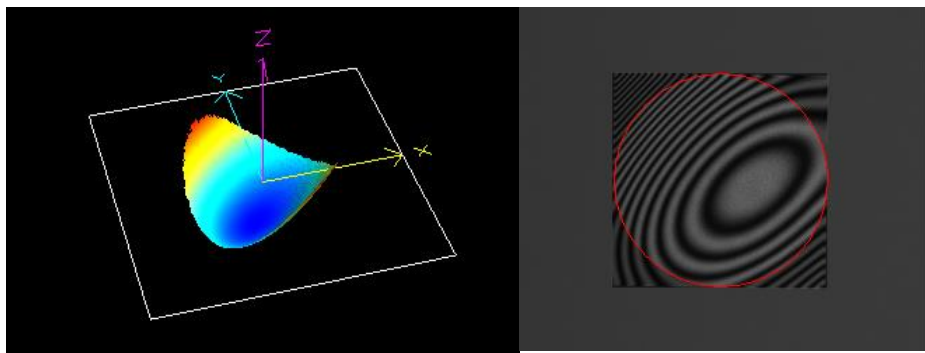


Fig. 8 (b). Surface contour over 4" diameter and interferogram of 4" square surface after grinding with A grit: PV 3.868 wv; RMS 0.9065 wv; Power 2.4931 wv.

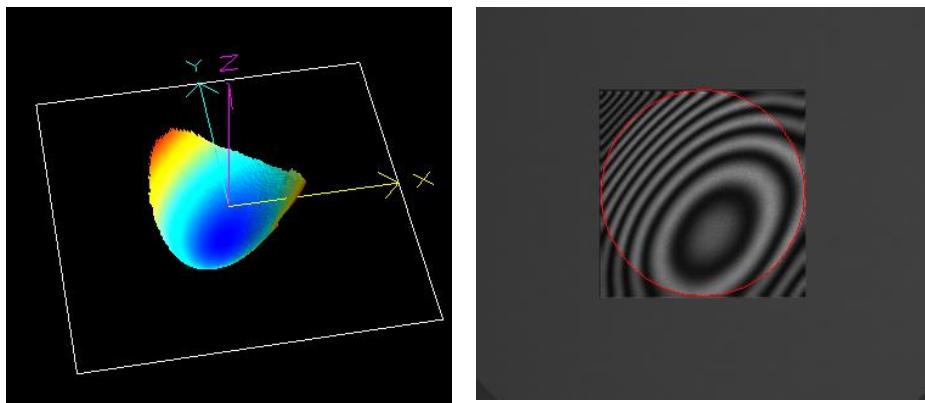


Fig. 8 (c). Surface contour over 4" diameter and interferogram of 4" square surface after grinding with C grit: PV 3.936 wv; RMS 0.7783 wv; Power 2.1284 wv.



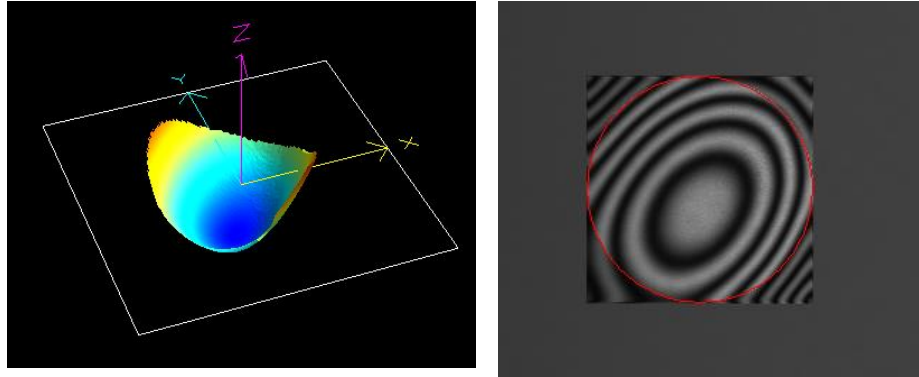


Fig. 8. (d). Surface contour over 4" diameter and interferogram of 4" square surface after grinding with E grit: PV 2.263 wv; RMS 0.4973 wv; Power 1.5330 wv.

Figure 9 shows a series of optical photomicrographs of a representative ground a-plane sapphire specimen showing the effects of different grit sizes on surface microstructure. It is clear from Figure 9 that the surface of the ground sample is covered with conchoidal fractures with a very high surface roughness compared to the pre-grinding condition.

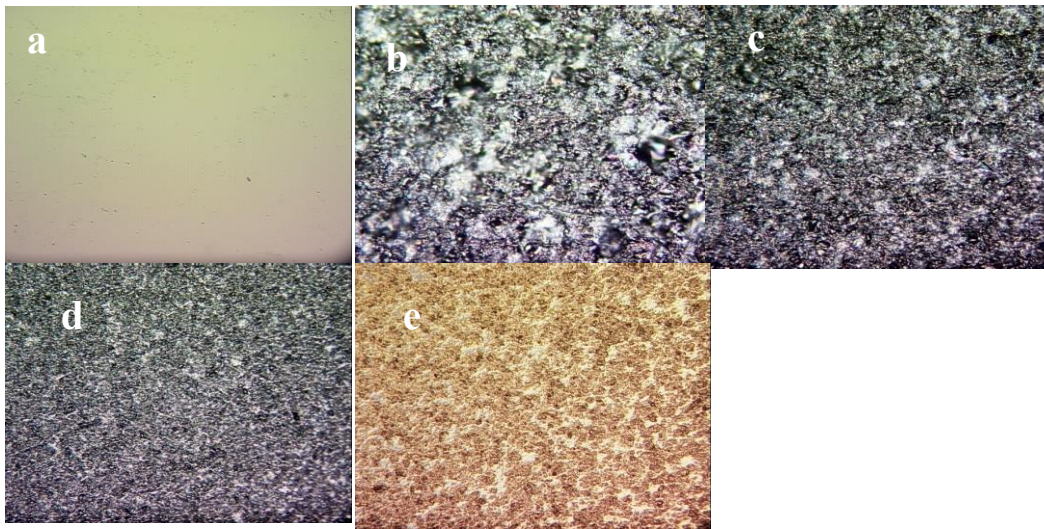


Fig. 9. Optical photomicrograph of a ground sample: (a) before grinding, (b) after A grit, (c) after B grit, (d) after C grit, (e) after D grit. (Magnification of 200X and  $A > B > C > D$ ) .

In general, the grinding operation is associated with sub-surface damage including micro-cracks and plastic deformation as reported above. Surface roughness is an indicator of the surface quality of the sample, and it is useful in approximating the depth of the sub-surface damage and, therefore, the amount of material to be removed in subsequent polishing steps. A close look at Figures 2b-2e reveal a progressive smoothing of the surface as the grit size decreases. This is consistent with the surface roughness result, as shown in Figure 10.

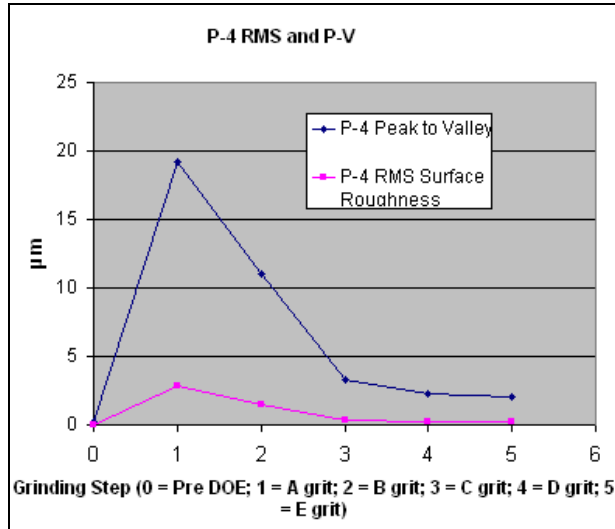


Fig. 10. Average RMS and peak-valley roughness for the ground sample in Figure 9.

Some clear trends were seen in the data. For example, the step-by-step relative change in stress, calculated via the Twyman effect, was very different for different fabrication processes as shown in Figure 11. For one grinding sequence, one sees a gradual stepwise reduction in stress that corresponds to the expected trend as grit size is reduced. Conversely, another process shows an inconsistent pattern of stress variation, indicating that sub-surface damage is not being removed in an orderly manner. In both cases, the same stepwise grit size reduction occurred so the difference must be due to the other parametric changes. This information will be used to guide subsequent process development activities.

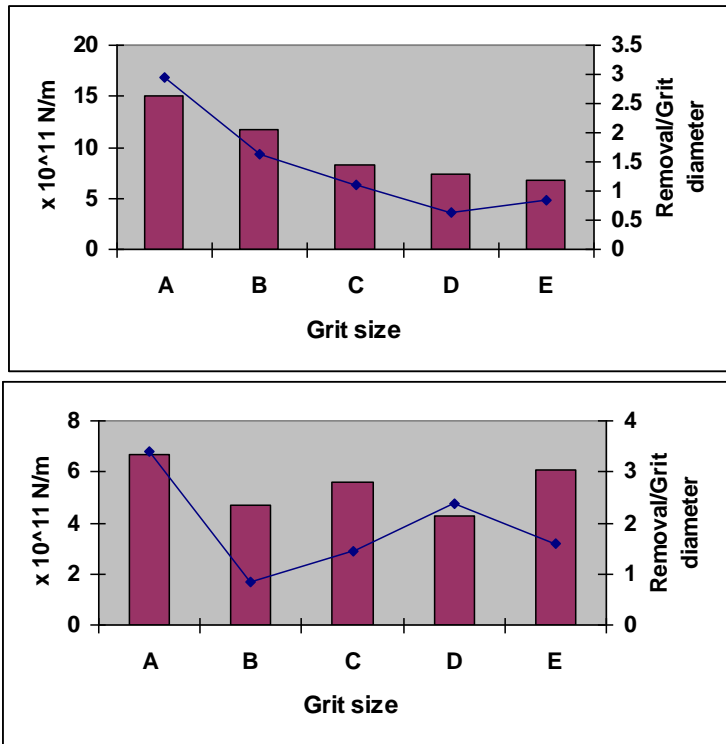


Fig. 11. Upper process exhibits a progressive reduction in stress as the grit size is reduced. Conversely, lower process exhibits an inconsistent pattern of stress variation.

## CONCLUSION

The technique of Raman / fluorescence spectroscopy using the frequency shift of the ruby lines was used to characterize grinding and polishing induced stress/surface damage in sapphire panels. The measurements performed on the various samples subjected to a unique set of grinding and polishing conditions show that the observed frequency shifts are different for each process, as expected. Depending on the specific process parameters and the position on the sample where the measurements were made, the shift/stress can either be compressive or tensile. This is related to the highly random nature of the loose abrasive process, the free movement of the irregular abrasive over the panel, and the nature and distribution of stress across the panel. The observed frequency shifts, within experimental resolution, are believed to be changes in local orientation and/or local interionic distance in the vicinity of the chromium ion as a result of fabrication process induced deformation such as dislocation and strain. This is supported by the observation of high densities of dislocations in the region of indentation by transmission electron microscopy studies,<sup>9,10</sup> observations of cracks, twins and dislocations on ground surfaces, and dislocations on polished surfaces,<sup>11</sup> and spatial variation in the stress within the vicinity of the indentation region.<sup>8</sup> Based on the present result, previous work and the work of others discussed above, it appears reasonable to conclude that this technique has a great potential as a quantitative and valuable tool for the characterization of surface stress and surface damage in sapphire panels.

The method based on optical birefringence did not demonstrate an ability to distinguish individual contributions to overall retardation due to thickness variation and residual stress. Based on these results, therefore, this technique in its current state is not suitable to provide accurate, consistent and reliable information that is useful in assessing the fabrication induced stress. More work is needed in this area to allow independent determination of crystal thickness accurately in order to extract the process-induced birefringence.

The Twyman effect may be used qualitatively to monitor relative stress and sub-surface damage in the production of sapphire panels.

## ACKNOWLEDGEMENT

This work was sponsored by the Office of the Naval Research (ONR) under Contract No. N00014-04-C-0419, and Air Force Research Laboratory (AFRL) under Contract No. FA 8650-05-D-5806/0004.

## REFERENCES

1. J.E. Greivenkamp, M. T. Chang, in *Optical fabrication and testing workshop*, 1992 Technical Digest Series, **24**, (OSA, Washington, DC 1992).
2. D. Harris, *Materials for Infrared Windows and Domes: Properties and Performance*, SPIE, Bellingham, WA, (1998).
3. Y. Zhou, P. D. Funkenbusch, D. J. Quesnel, D. Golini and A. Lindquist, "Effects of etching and imaging mode on the measurement of subsurface damage in microground optical glasses" *J. Am. Ceram. Soc.* **77** (12) 3277-80 (1994).
4. L. Grabner, "Spectroscopic Technique for the measurement of residual Stress in Sintered Al<sub>2</sub>O<sub>3</sub>" *J. Appl. Phys.*, **49** (2) 580-83 (1978).
5. Q. Ma and D. R. Clark, "Piezospectroscopic Determination of Residual Stresses in Polycrystalline Alumina" *J. Am. Ceram. Soc.* **77** (2) 298-302 (1994).
6. J. He and D. R. Clarke, "Determination of the Piezospectroscopic Coefficient for Chromium-Doped Sapphire" *J. Am. Ceram. Soc.* **78** (5) 1347-1353 (1994).
7. S. M. Sharma and Y. M. Gupta, "Theoretical analysis of R-line shifts of ruby subjected to different deformation conditions" *Phys. Rev. B*, **43**, (1), 879-893 (1991).
8. S. E. Molis and D. R. Clarke, "Measurement of Stress using Fluorescence in an Optical Microprobe: Stresses around Indentations in a Chromium-Doped sapphire" *J. Am. Ceram. Soc.* **73** (11) 3189-94 (1990).

9. B. J. Hockey, "Plastic Deformation of Aluminum Oxide by Indentation and Abrasion" J. Am. Ceram. Soc. **54** (5) 223-231 (1971).
10. H. M. Chan and B. R. Lawn, "Indentation Deformation and Fracture of Sapphire" J. Am. Ceram. Soc. **71** (1) 29-35 (1988).
11. D. Black, R. Polvani, L. Braun, B. Hockey and G. White, "Detection of sub-surface damage: studies in sapphire" SPIE Vol. **3060**, 102-114 (1997).